Localization of Electronic Excitations in Conjugated Polymers Studied by DFT

Iffat H. Nayyar,[†,§,⊥] Enrique R. Batista,[†] Sergei Tretiak,*[,†,‡] Avadh Saxena,[†] D. L. Smith,[†] and Richard L. Martin[†]

[†]Theoretical Division and Center for Nonlinear Studies and [‡]Center for Integrated Nanotechnologies, Los Alamos National Laboratory, Los Alamos, New Mexico 87545, United States
[§]NanoScience Technology Center and [⊥]Department of Physics, University of Central Florida, Orlando, Florida 32826, United States

ABSTRACT: We present an extensive density functional theory (DFT) study on the neutral and charged electronic excitations in oligophenylene vinylenes including lowest singlet (S_1) and triplet (T_1) excitons and positive (P^+) and negative (P^-) polarons. We investigated the vibrational and electronic properties of molecules using five different DFT functionals from pure GGA to long-range-corrected hybrids and found an explicit correlation between the spatial extent of the state and the fraction of the orbital exchange. While solvent effects are found to be negligible for neutral (S_1 and T_1) excitons, they play an important role for charged (P^+ and P^-) species. S_1 states are observed to be spatially less localized compared to the polaronic wave functions (P^+ and P^-). This is in contrast to the T_1 states, which exhibit more spatial confinement in comparison to P^+ and P^- states.

SECTION: Dynamics, Clusters, Excited States
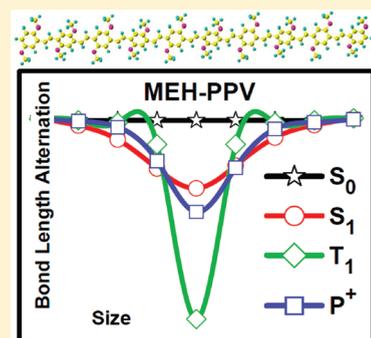
Charged excitations like polarons and neutral singlet and triplet excitons are responsible for electronic transport in π-conjugated organic polymers. These polymers find a variety of applications in optical devices such as field-effect transistors,[1] photovoltaic cells,[2] organic light-emitting diodes,[3] laser materials,[4] and solar cells.[5] Three kinds of excitation processes play a vital role in the development of organic optoelectronics: [6] charge transfer by an electron or a hole (polaron) in the polymer and excitonic energy transfer following the recombination of an electron and a hole, producing singlet and triplet excitations. Therefore, a detailed understanding of the role of neutral and charged excitations in the mechanism of the intense electroluminescence and charge transport[7] is critical for improving the efficiency of these polymer-based devices.[8] Among the organic polymers, derivatives of PPV [poly(p-phenylene vinylene)] such as MEH-PPV [poly{2-methoxy-5-(2-ethyl-hexyloxy)PPV}] are the candidates of choice for potential use in these optical devices, owing to the ease and small cost of processing, their electronic and structural flexibility, and superior luminescent properties.[9] The easy availability of the spectroscopic measurements and experimental evidence[10−12] of self-localization in these polymers can be further exploited to explore the underlying physics of the spin coupling and spintronics[13] using computational quantum chemistry.

Earlier investigations on charged excitations in polythiophenes have shown that the unrestricted Hartree−Fock (UHF) method is not suited for studying open-shell π-conjugated systems due to inherent spin contamination.[14] The restricted open-shell HF (ROHF) calculations performed on thiophene oligomer radical cations exhibited localized character of the polaronic defects.[14,15]

For comparison, a generalized gradient approximation (GGA) functional, BLYP used within the unrestricted Kohn−Sham (UKS) scheme, was unable to produce charge localization.[14] In a study by Zuppiroli et al,[16] pure DFT overestimated the charge delocalization, whereas the semiempirical (AM1) calculations were successful in describing the polaronic character of the charged carriers. In contrast, hybrid DFT calculations with 50% of the orbital exchange component yielded a localized polaron.[17] Time-dependent DFT (TD-DFT) calculations of PPV oligomers emphasized the importance of the hybrid component in the functional model for correct description of excitonic properties.[18,19] Semiempirical calculations of singlet excitons provided a detailed analysis of exciton dynamics and self-trapping in PPV and polyfluorenes.[20,21]

Recent investigations[22,23] of spin response in π-conjugated polymer films elucidated the role of hyperfine interactions (HFI) in various organic magnetoelectronic devices and the influence of hydrogen isotope exchange in MEH-PPV on the magnetic response of spin-dependent processes. This allowed experimental evaluation of the polaronic spin density in MEH-PPV to be spread over two to three repeat units (about 10 C—H bonds). This motivated us to perform the present DFT study to benchmark the ability of current functional models to describe the spatial extent of self-trapped neutral and charged electronic excitations in these systems. We have investigated the vibrational and electronic properties of the MEH-PPV oligomer (top panel
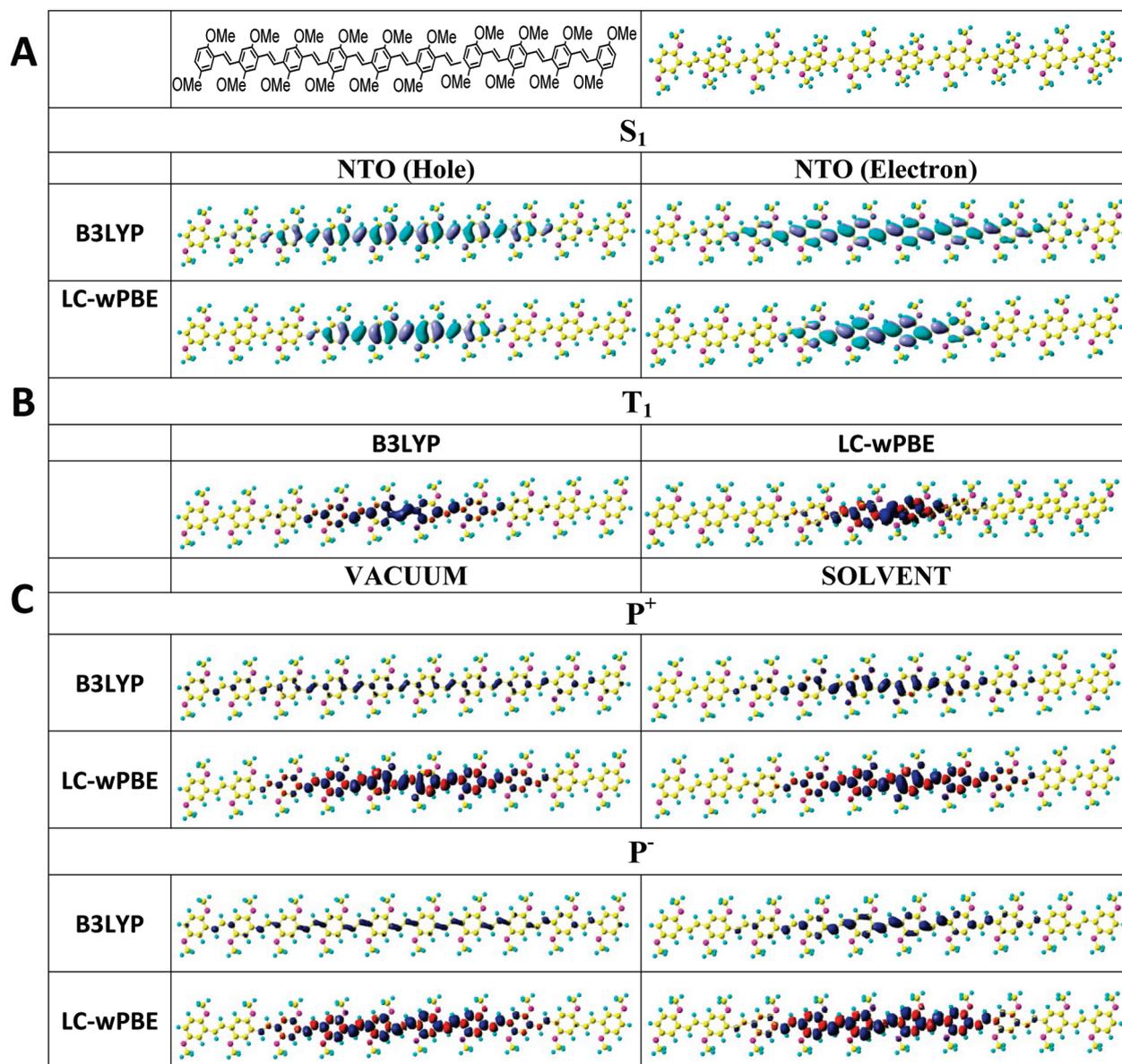
Figure 1. (A) The top panels display the MEH-PPV oligomer consisting of 10 repeat units. Orbital plots show NTOs for the hole and electron for the first singlet excited state (S_1) calculated at B3LYP/6-31G* and LC-wPBE/6-31G* optimized levels. (B) Orbital plots show the Mulliken atomic spin density distribution for the first triplet excited state (T_1) calculated at B3LYP/6-31G* and LC-wPBE/6-31G* optimized levels. (C) Orbital plots show the Mulliken atomic spin density distribution for positive polaronic (P^+) and negative polaronic (P^-) species calculated at B3LYP/6-31G* and LC-wPBE/6-31G* optimized levels.

in Figure 1A) using several modern density functionals. In addition to the ground state (charge = 0, spin = 0) denoted as S_0, we considered four electronic excitations, namely, the first singlet excited state S_1 (charge = 0, spin = 0), first triplet excited state T_1 (charge = 0, spin = 1), and positive P^+ (charge = +1, spin = 1/2) and negative P^- (charge = −1, spin = 1/2) polarons. Cationic P^+ and anionic P^- species correspond to the presence of a hole and an electron on the chain, respectively. Fully relaxed geometries of all five states (S_0, S_1, T_1, P^+, and P^-) have been obtained using five different DFT functionals without imposing any symmetry constraints. In particular, we used DFT models ranging from pure GGA to long-range-corrected hybrids, namely, PBE[24] ($a = 0$), B3LYP[25] ($a = 20$), BHandHLYP[25] ($a = 50$), CAM-B3LYP[26] ($a = 20-65$), and LC-wPBE

($a = 0-100$),[27] where parameter a is the fraction of HF exchange in the exchange-correlation (XC) functional given as

$$E_{XC} = aE_X^{HF} + (1 - a)E_X^{GGA} + E_C^{GGA} \qquad (1)$$

The long-range-corrected functionals behave as typical hybrid or GGA at short range. However, they have increasing HF component at longer distances up to a maximum value, 65% for CAM-B3LYP and 100% for LC-wPBE. To explore the effects of a polymer's highly polarizable dielectric environment, we use the conductor-like polarizable continuum model (CPCM) and a moderately polar solvent, acetonitrile ($\varepsilon = 37.5$), as implemented in Gaussian09 software package.[28] Optimal geometries of S_0, T_1, P^+, and P^- states have been obtained using the standard

567

dx.doi.org/10.1021/jz101740w |*J. Phys. Chem. Lett.* 2011, 2, 566–571

self-consistent force (SCF) scheme, whereas S_1 has been calculated using TD-DFT methodology. All of the computations were performed using the Gaussian09 suite[28] and the 6-31G* basis set.

The top panel in Figure 1A depicts the 10 repeat units of the MEH-PPV oligomer in its trans-isomeric geometrical form (alternate up and down dihedrals along the backbone of the chain). Each repeat unit consists of a phenyl ring attached to a vinylene linkage. The last two repeat units share the vinyl bridge. In our model, the side-chain groups OC_8H_{17} in MEH-PPV have been replaced by OCH_3 to speed up the quantum calculations. The other panels in Figure 1A show characteristic natural transition orbitals (NTOs) for the hole and electron of the photoexcited S_1 excitons. The NTO analysis allows for orbital representation of the electronic transition density matrix.[29] Figure 1B represents selected atomic spin density distributions for T_1 states, whereas Figure 1C includes these distributions for P^+ and P^- species. NTOs and spin distributions are calculated using two DFT models, one with a low fraction of HF exchange (B3LYP) and the other one with full HF exchange at long range (LC-wPBE).

The orbital and spin distributions clearly emphasize the localization of electronic excitations at their fully relaxed excited-state geometries in the middle of the chain with the higher fraction of orbital exchange in DFT functionals. Inclusion of the dielectric environment also tends to increase the localization of the charged species (P^+ and P^-). These observations will be explained in much greater detail in the following sections. Therefore, in this study, we emphasize the crucial role played by the amount of long-range orbital exchange in the density functional and the surrounding dielectric medium in studying the spatial confinement of the wave functions in accordance with experimental studies performed in these polymers. Interestingly, unsubstituted PPV was found to behave very similarly to MEH-PPV in its trans-isomeric form. Hence, we chose only to discuss MEH-PPV hereafter. As expected, we found negligible effects of the dielectric environment on the properties of neutral states S_0, S_1, and T_1, and hereafter, we will discuss only gas-phase calculations of these excitations.

Neutral excitations and the injection of an excess charge or spin into organic polymers relax the lattice geometry and electronic orbitals over the limited section of the π-conjugated chain due to their strong electron—phonon coupling. To quantify this phenomenon, we use one geometric parameter, namely, the bond length alternation (BLA) defined as the difference between carbon—carbon single and double bond lengths in the vinyl linkage along the backbone of the polymer. BLA is a useful parameter in predicting the degree of localization of distortion in conjugated molecular chains.[21] Charge or spin density distributions are other helpful tools to estimate the spatial extent of the excitation.

Figure 2 shows the calculated BLA along the chain for all states in question (S_0, S_1, T_1, P^+, and P^-). For the neutral ground state geometry (S_0), we observe an overall increase in the BLA corresponding to the increase in the fraction of HF exchange uniform over all of the repeat units, which promotes Peierls dimerization in the π-electron systems. The BHandHLYP with 50% exchange is close to the CAM-B3LYP (20−65%). LC-wPBE (0−100%) exhibits the highest overall BLA compared to other XC functionals considered. For S_1 excitation, we find an explicit correlation between the degree of localization and the percent of HF component in the functionals. The rings at either

end of the polymer chains are not perturbed with this exciton; their BLA is almost identical to the one found in the corresponding neutral polymer at its ground state S_0 optimized at the same level of theory. As we proceed to the middle of the chain from both ends, the C—C bond length of the vinylene linkage keeps decreasing (intermediate to C—C and C=C), whereas the C=C bond length keeps increasing, and the BLA reaches its minimum exactly at the middle of the chain, signifying the self-trapping of the exciton.[21] Pure GGA functional PBE fails to exhibit the spatial confinement of the wave function. A small fraction (20%) of the HF exchange starts to localize the excitation. However, BHandHLYP, CAM-B3LYP, and LC-wPBE exhibit clear structural localization, the sizes of the self-trapped excitation ranging from three to four repeat units. This is in agreement with a joint experimental and theoretical study,[30] in which the lattice deformations for S_1 states are reported to extend over a length of about 20 Å (between three and four repeat units). The T_1 states are much more spatially localized compared to S_1 excitations. This is also observed in Karabunarliev et al.'s study[31] and argued due to the absence of repulsive spin-exchange between the electron and hole. Localization in the B3LYP geometry is much more pronounced than that for S_1. However, BHandHLYP, CAM-B3LYP, and LC-wPBE optimized structures lead to an inverted BLA (the C—C bond being shorter than the C=C bond in the center), resulting in a much more localized T_1 state compared to the B3LYP data (see Figures 2 and 1B). Here, T_1 is found to be spatially confined between one and two repeat units in the middle of the chain.

For the P^+ state, like for neutral excitations, we find an enhancement in the phonon-induced self-trapping with increasing orbital exchange fraction. Although, BHandHLYP and CAM-B3LYP exhibit the structural localization (see Figures 2 and 1C), these models are still inefficient in reproducing the experimentally observed polaron size.[22] However, PBE and B3LYP completely fail to predict the polaron formation. Long-range-corrected LC-wPBE has the sharpest minimum at the middle of the chain and extends over two to three repeat units, in accordance with experimental observations.[22] Hence, it is evident that the application of asymptotically corrected hybrid DFT functionals is critical in order to predict the polaron formation. Surprisingly, the P^+ state is less localized than the T_1 state. P^+ and P^- excitations display very similar trends (P^- is not shown in Figure 2).

Thus, we can state that particle—hole symmetry is preserved in the trans-isomeric form of the polymer. However, we have noticed the differences for P^+ and P^- excitations after introduction of certain defects in the chain (to be published elsewhere), which is consistent with experimental observation[23] indicating the difference in the P^+ and P^- polaron sizes.

We find no substantial change in the BLA of the neutral oligomer (S_0) and neutral excitations (S_1 and T_1) by the inclusion of a polarizable medium through solvent calculations as compared to the corresponding gas-phase results. This is consistent with earlier DFT studies on the effect of the polarization function on large systems with relatively long and easily polarizable π-bridges.[32,33] However, as shown in Figure 2, polar solvent tends to increase the geometric distortion for all of the XC functionals used whether pure GGA, hybrid, or long-range-corrected, in comparison to that in vacuum for charged species (P^+ and P^-). One of the major observations here is that the polarization of the medium has an effect on the polymer properties, similar to adding long-range corrections to hybrid

568

dx.doi.org/10.1021/jz101740w |J. Phys. Chem. Lett. 2011, 2, 566–571
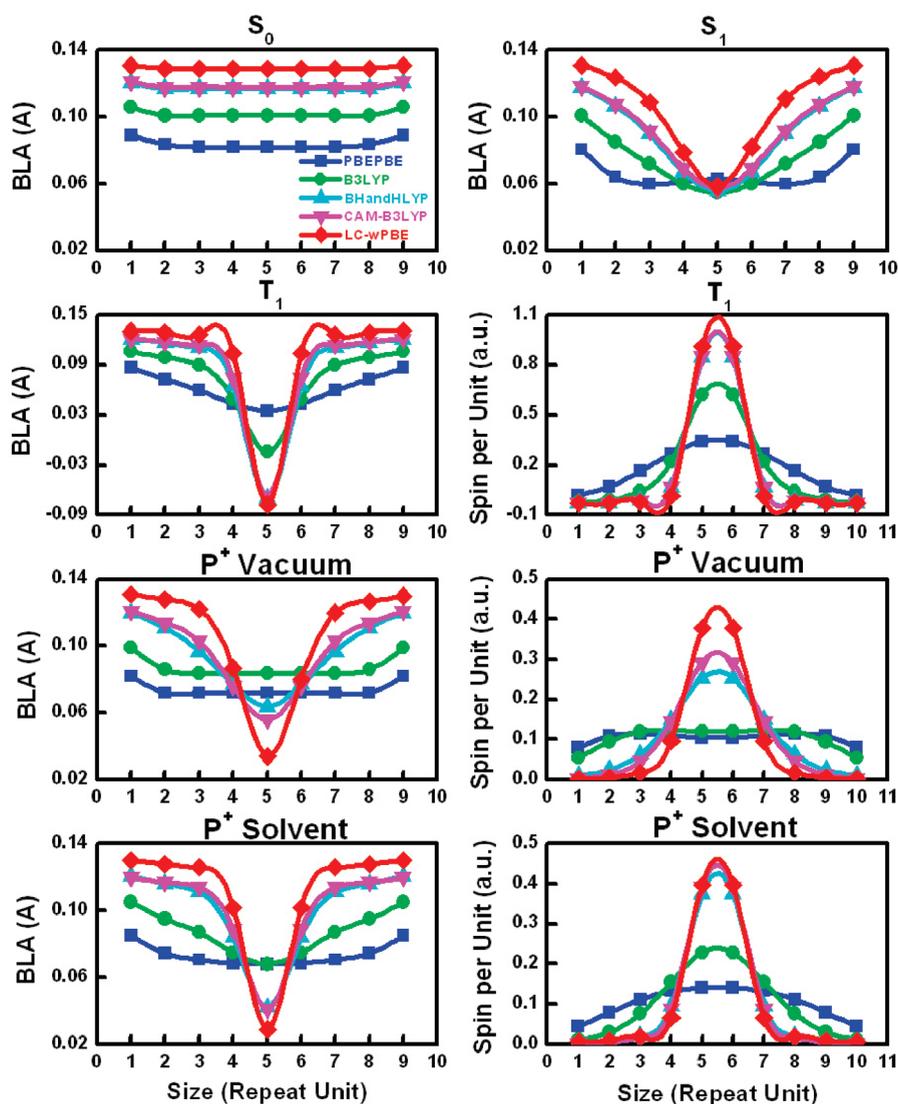
Figure 2. BLA (Å) of vinylene units (left) and Mulliken atomic spin densitites (au) per repeat unit (right) of the MEH-PPV oligomer computed using PBE, B3LYP, BHandHLYP, CAM-B3LYP, and LC-wPBE functional models, and the 6-31G* basis set. Geometry optimization is carried out for five different electronic states, the ground state (S_0), the first singlet excited state (S_1), the first triplet excited state (T_1), the positive polaron (P^+), and negative polaron (P^-). The Mulliken atomic spin densities (spin per unit) are obtained by performing SCF calculations for T_1, P^+, and P^- excitations in their corresponding fully relaxed geometries.

DFT. It is clearly evident from the BLA pattern of P^+ excitation that a small fraction of HF exchange (20%) in the XC functional, which was unable to predict the structural distortion in the absence of a polarizing medium, begins to exhibit the localization properties in its presence. BHandHLYP and CAM-B3LYP manifest significant changes with respect to geometry localization in the presence of the solvent compared to that for their corresponding gas-phase geometries. It is interesting to note that BHandHLYP results are almost similar to CAM-B3LYP results and very close to LC-wPBE results. In the dielectric medium, LC-wPBE is able to predict the polaron sizes correctly, in accordance with the experiment extending around two repeat units. This implies that inclusion of a polarizable dielectric medium has a greater effect on the spatial confinement of the polaronic wave functions, in addition to long-range corrections to DFT functionals. The BLA patterns for P^- states in the presence of solvent are the same as those of P^+.

We also examine the Mulliken atomic spin densities (difference in the spin of electrons in alpha and beta molecular orbitals) integrated over each repeat unit for T_1, P^+, and P^- excitations. These quantities shown in Figure 2 are complementary to BLA and show a similar order of localization in both the gas phase and solvent. Comparison of these two quantities, BLA signifying localization via geometric distortion and spin density distribution probing localization of the electronic density, allows one to distinguish between two distinct origins leading to localization of electronic excitations, spatial localization of the state wave function by itself on the undistorted geometry and localization of the wave function assured by distortion of the structure during geometry relaxation. We found (not shown) that neutral excitations S_1 and T_1 localize primarily due to geometric distortion (depicted in the BLA functional form in Figure 2). In contrast, charged species P^+ and P^- mainly localize due to electronic reasons. This is in agreement with the
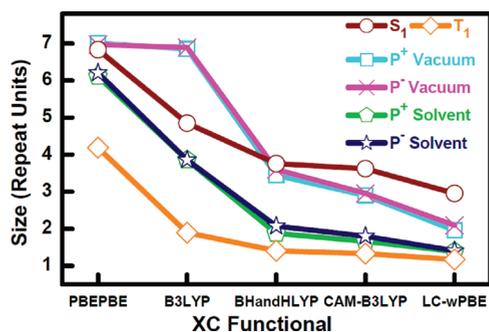
Figure 3. Characteristic size of the electronic excitations defined as the full width at half-maximum (fwhm) in terms of repeat units of the BLA extent in the MEH-PPV oligomer calculated for S_1, T_1, P^+, and P^- states from Figure 2 data.

observations elucidated in Geskin et al.[34] about the emphasis on the choice of the method for electronic structure calculations rather than geometrical optimization for charged species. This suggests that, for charged excitations, localization is principally produced by the electronic rearrangements and the character of the functional rather than the structural distortions; however, the opposite seems to be the case for neutral excitons. A detailed analysis of these phenomena will be presented elsewhere.

Finally, we summarize the localization properties predicted by different DFT functionals in terms of the characteristic size of the electronic excitations under study in Figure 3. This size is defined as the full width at half-maximum (fwhm) in terms of repeat units of the optimized carbon—carbon BLA of vinylene bridges of the polymer chain. For P^+ and P^- states in solvent, LC-wPBE, CAM-B3LYP, and BHandHLYP predict the localization in agreement with experimental findings.[22] Particle—hole symmetry is clearly evident from this figure. The S_1 states of neutral oligomers are spatially less localized compared to polaronic wave functions, whereas T_1 excitations are more localized than them.

Poly(phenylene vinylene)-based materials are of substantial theoretical interest for the extensive available experimental data[11,35−37] and significant technological promise. We investigated theoretically the five electronic states (S_0, S_1, T_1, P^+, and P^-) in MEH-PPV oligomer playing the major role in the charge and energy-transfer dynamics in the bulk polymeric materials. It has been established that the long-range corrections to the XC functional are crucial in order to predict the spatial localization of all electronic excitations considered. Inclusion of dielectric medium effects is also shown to be important for the polaron formation. LC-wPBE (0−100%) predicts the polaron localization in both vacuum and solvent agreeing with experimental data for charged polymers, whereas BHandHLYP (50%) and CAM-B3LYP (20−65%) produce significant localization only in the presence of a polarizable solvent.

AUTHOR INFORMATION

Corresponding Author
*E-mail: serg@lanl.gov.

ACKNOWLEDGMENT

REFERENCES

(1) Rasul, A.; Zhang, J.; Gamota, D.; Singh, M.; Takoudis, C. Flexible High Capacitance Nanocomposite Gate Insulator for Printed Organic Field-Effect Transistors. *Thin Solid Films* **2010**, *518*, 7024–7028.

(2) Sun, S. Y.; Salim, T.; Wong, L. H.; Foo, Y. L.; Boey, F.; Lam, Y. M. A New Insight into Controlling Poly(3-hexylthiophene) Nanofiber Growth through a Mixed-Solvent Approach for Organic Photovoltaics Applications. *J. Mater. Chem.* **2011**, *21*, 377–386.

(3) He, Z.; Kan, C. W.; Ho, C. L.; Wong, W. Y.; Chui, C. H.; Tong, K. L.; So, S. K.; Lee, T. H.; Leung, L. M.; Lin, Z. Y. Light-Emitting Dyes Derived from Bifunctional Chromophores of Diarylamine and Oxadiazole Synthesis, Crystal Structure, Photophysics and Electroluminescence. *Dyes Pigm.* **2011**, *88*, 333–343.

(4) Mayoral, M. J.; Ovejero, P.; Cano, M.; Orellana, G. Alkoxy-Substituted Difluoroboron Benzoylmethanes for Photonics Applications: A Photophysical and Spectroscopic Study. *Dalton Transactions* **2011**, *40*, 377–383.

(5) Liu, Q. S.; Jiang, K. J.; Guan, B.; Tang, Z. M.; Pei, J. A.; Song, Y. L. A Novel Bulk Heterojunction Solar Cell Based on a Donor—Acceptor Conjugated Triphenylamine Dye. *Chem. Commun.* **2011**, *47*, 740–742.

(6) Ran, G. Z.; Jiang, D. F.; Kan, Q.; Chen, H. D. Experimental Observation of Polarized Electroluminescence from Edge-Emission Organic Light Emitting Devices. *Appl. Phys. Lett.* **2010**, *97*, 233304.

(7) Hoyer, U.; Wagner, M.; Swonke, T.; Bachmann, J.; Auer, R.; Osvet, A.; Brabec, C. J. Electroluminescence Imaging of Organic Photovoltaic Modules. *Appl. Phys. Lett.* **2010**, *97*, 233303.

(8) Kim, H. N.; Guo, Z. Q.; Zhu, W. H.; Yoon, J.; Tian, H. Recent Progress on Polymer-Based Fluorescent and Colorimetric Chemosensors. *Chem. Soc. Rev.* **2011**, *40*, 79–93.

(9) Ponomarenko, S. A.; Kirchmeyer, S. Conjugated Organosilicon Materials for Organic Electronics and Photonics. *Silicon Polymers* **2011**, *235*, 33–110.

(10) Frankevich, E.; Nishihara, Y.; Fujii, A.; Ozaki, M.; Yoshino, K. Time-Resolved Study of Polaron Pairs in Conjugated Polymers by Two-Correlated-Pulses Technique. *Phys. Rev. B* **2002**, *66*, 155203/1–155203/7.

(11) Moses, D.; Dogariu, A.; Heeger, A. J. Ultrafast Detection of Charged Photocarriers in Conjugated Polymers. *Phys. Rev. B* **2000**, *61*, 9373–9379.

(12) Kuroda, S.; Marumoto, K.; Shimoi, Y.; Abe, S. ESR Spectroscopy of Polarons in Conjugated Electroluminescent Polymers. *Thin Solid Films* **2001**, *393*, 304–309.

(13) Drew, A. J.; Hoppler, J.; Schulz, L.; Pratt, F. L.; Desai, P.; Shakya, P.; Kreouzis, T.; Gillin, W. P.; Suter, A.; Morley, N. A. et al. Direct Measurement of the Electronic Spin Diffusion Length in a Fully Functional Organic Spin Valve by Low-Energy Muon Spin Rotation. *Nat. Mater.* **2009**, *8*, 109–114.

(14) Moro, G.; Scalmani, G.; Cosentino, U.; Pitea, D. On the Structure of Polaronic Defects in Thiophene Oligomers: a Combined Hartree—Fock and Density Functional Theory Study. *Synth. Met.* **2000**, *108*, 165–172.

(15) Geskin, V. M.; Cornil, J.; Bredas, J. L. Comment on 'Polaron Formation and Symmetry Breaking' by L Zuppiroli et al. *Chem. Phys. Lett.* **2005**, *403*, 228–231.

(16) Zuppiroli, L.; Bieber, A.; Michoud, D.; Galli, G.; Gygi, F.; Bussac, M. N.; Andre, J. J. Polaron Formation and Symmetry Breaking. *Chem. Phys. Lett.* **2003**, *374*, 7–12.

(17) Geskin, V. M.; Dkhissi, A.; Bredas, J. L. Oligothiophene Radical Cations: Polaron Structure in Hybrid DFT and MP2 Calculations. *Int. J. Quantum Chem.* **2003**, *91*, 350–354.

570

dx.doi.org/10.1021/jz101740w |*J. Phys. Chem. Lett.* 2011, 2, 566–571

(18) Igumenshchev, K. I.; Tretiak, S.; Chernyak, V. Y. Excitonic Effects in a Time-Dependent Density Functional Theory. *J. Chem. Phys.* **2007**, *127*, 114902(10).

(19) Tretiak, S.; Igumenshchev, K.; Chernyak, V. Y. Exciton Sizes of Conducting Polymers Predicted by Time-Dependent Density Functional Theory. *Phys. Rev. B* **2005**, *71*, 033201(4).

(20) Franco, I.; Tretiak, S. Electron-Vibrational Dynamics of Photoexcited Polyfluorenes. *J. Am. Chem. Soc.* **2004**, *126*, 12130–12140.

(21) Tretiak, S.; Saxena, A.; Martin, R. L.; Bishop, A. R. Conformational Dynamics of Photoexcited Conjugated Molecules. *Phys. Rev. Lett.* **2002**, *89*, 097402(4).

(22) Nguyen, T. D.; Hukic-Markosian, G.; Wang, F. J.; Wojcik, L.; Li, X. G.; Ehrenfreund, E.; Vardeny, Z. V. Isotope Effect in Spin Response of π-Conjugated Polymer Films and Devices. *Nat. Mater.* **2010**, *9*, 345–352.

(23) McCamey, D. R.; van Schooten, K. J.; Baker, W. J.; Lee, S. Y.; Paik, S. Y.; Lupton, J. M.; Boehme, C. Hyperfine-Field-Mediated Spin Beating in Electrostatically Bound Charge Carrier Pairs. *Phys. Rev. Lett.* **2010**, *104*, 017601(4).

(24) Perdew, J. P.; Burke, K.; Ernzerhof, M. Errata: Generalized Gradient Approximation Made Simple [Phys. Rev. Lett. 77, 3865 (1996)]. *Phys. Rev. Lett.* **1997**, *77*, 1396–1396.

(25) Becke, A. D. A New Mixing of Hartree—Fock and Local Density-Functional Theories. *J. Chem. Phys.* **1993**, *98*, 1372–1377.

(26) Yanai, T.; Tew, D. P.; Handy, N. C. A New Hybrid Exchange-Correlation Functional Using the Coulomb-Attenuating Method (CAM-B3LYP). *Chem. Phys. Lett.* **2004**, *393*, 51–57.

(27) Tawada, Y.; Tsuneda, T.; Yanagisawa, S.; Yanai, T.; Hirao, K. A Long-Range-Corrected Time-Dependent Density Functional Theory. *J. Chem. Phys.* **2004**, *120*, 8425–8433.

(28) Frisch, M. J.; Trucks, G. W.; Schlegel, H. B.; Scuseria, G. E.; Robb, M. A.; Cheeseman, J. R.; Scalmani, G.; Barone, V.; Mennucci, B.; Petersson, G. A. et al. *Gaussian 09*, revision A.1; Gaussian Inc.: Wallingford, CT, 2009.

(29) Martin, R. L. Natural Transition Orbitals. *J. Chem. Phys.* **2003**, *118*, 4775–4777.

(30) Cornil, J.; Beljonne, D.; Heller, C. M.; Campbell, I. H.; Laurich, B. K.; Smith, D. L.; Bradley, D. D. C.; Mullen, K.; Bredas, J. L. Photoluminescence Spectra of Oligo-Paraphenylenevinylenes: A Joint Theoretical and Experimental Characterization. *Chem. Phys. Lett.* **1997**, *278*, 139–145.

(31) Karabunarliev, S.; Bittner, E. R. Polaron—Excitons and Electron-Vibrational Band Shapes in Conjugated Polymers. *J. Chem. Phys.* **2003**, *118*, 4291–4296.

(32) Suponitsky, K. Y.; Masunov, A. E.; Antipin, M. Y. Computational Search for Nonlinear Optical Materials: Are Polarization Functions Important in the Hyperpolarizability Predictions of Molecules and Aggregates?. *Mendeleev Commun.* **2009**, *19*, 311–313.

(33) Masunov, A.; Tretiak, S.; Hong, J. W.; Liu, B.; Bazan, G. C. Theoretical Study of the Effects of Solvent Environment on Photophysical Properties and Electronic Structure of Paracyclophane Chromophores. *J. Chem. Phys.* **2005**, *122*, 224505(10).

(34) Geskin, V. M.; Grozema, F. C.; Siebbeles, L. D. A.; Beljonne, D.; Bredas, J. L.; Cornil, J. Impact of the Computational Method on the Geometric and Electronic Properties of Oligo(phenylene vinylene) Radical Cations. *J. Phys. Chem. B* **2005**, *109*, 20237–20243.

(35) Brabec, C. J.; Winder, C.; Scharber, M. C.; Sariciftci, N. S.; Hummelen, J. C.; Svensson, M.; Andersson, M. R. Influence of Disorder on the Photoinduced Excitations in Phenyl Substituted Polythiophenes. *J. Chem. Phys.* **2001**, *115*, 7235–7244.

(36) Nishihara, Y.; Frankevich, E.; Fujii, A.; Ozaki, M.; Yoshino, K. Properties of Polaron Pairs in Conjugated Polymers Studied by Two-Correlated-Pulses Technique. *J. Phys. Soc. Jpn.* **2004**, *73*, 1888–1894.

(37) Wei, X.; Hess, B. C.; Vardeny, Z. V.; Wudl, F. Studies of Photoexcited States in Polyacetylene and Poly(paraphenylenevinylene) by Absorption Detected Magnetic-Resonance — The Case of Neutral Photoexcitations. *Phys. Rev. Lett.* **1992**, *68*, 666–669.

571

dx.doi.org/10.1021/jz101740w |*J. Phys. Chem. Lett.* 2011, 2, 566–571